Height Recovery From Intensity Gradient*

Ruo Zhang and Mubarak Shah
Computer Science Department
University of Central Florida
Orlando, FL 32816
shah@cs.ucf.edu

Abstract

Unlike existing global shape-from-shading algorithms which involve the brightness constraint in their formulation, we propose a new algorithm which replaces the brightness constraint by an intensity gradient constraint. This is a global approach which obtains the solution by the minimization of an error function over the entire image. Through the linearization of the reflectance map and the discretization of the surface gradient, the intensity gradient can be expressed as a linear function of the surface height. A quadratic error function, which involves the intensity gradient constraint and the traditional smoothness constraint, is minimized efficiently by solving a sparse linear system using the multigrid technique. Neither the information at singular points nor the information at occluding boundaries is needed for the initialization.

1 Introduction

The goal of shape-from-shading (SFS) is to reconstruct the 3-D shape of an object from its 2-D intensity image, assuming a proper reflectance map, which models the relationship between the intensity and surface shape, is given. Surface shape can be represented by height, gradient, normal, slant and tilt, or curvature. Since the reflectance map is a nonlinear equation in terms of the shape, simplifications are needed in order to restrict the problem. The first simplification, which is also the biggest for most SFS algorithms, is the assumption of diffuse reflection: Surfaces reflect light equally in all directions. The second simplification assumes the illumination is from a point light source at infinity. Other simplifications include assuming a known viewing direction, known light source direction, and orthographic projection. Together, these assumptions introduce a simple Lambertian model, which describes the intensity in terms of the cosine value of the angle between the surface normal and the light source direction. This model allows for the use of the information at singular points, and occluding boundaries. In order to obtain a correct solution for SFS, the local spherical assumption [8], the brightness constraint [1, 2, 3, 4, 5, 6, 7, 9, 10, 12, 13, 15, 17, 18], the brightness derivative constraint [18], the smoothness constraint [2, 4, 5, 6, 7, 9, 15], and the integrability constraint [5, 6, 15, 18], are used in addition to the information at singular points and occluding boundaries [1, 2, 3, 4, 5, 10, 15].

The spherical assumption approximates the local surface by a spherical patch. The brightness constraint minimizes the error between the reconstructed intensity and the input intensity, and the brightness derivative constraint minimizes the error between the reconstructed intensity derivatives and the input intensity derivatives. The smoothness constraint requires that the reconstructed surface be smooth. The integrability constraint ensures an integrable surface.

2 Previous Work

There are several simple and efficient SFS approaches which derive shape from local intensity information. These include methods by Pentland [12, 13], Lee & Rosenfeld [8], and Tsai & Shah [17].

Pentland [13] solved for the surface slant and tilt, the radius of curvature, and the light source direction using six equations obtained from the intensity, as well as the first and second derivatives of the intensity. His approach can classify a surface into one of five categories: Planar, cylindrical, convex, concave, or saddle surface. However, it is limited to surfaces with equal-magnitude principal curvatures.

Lee & Rosenfeld [8] considered the derivatives of the intensity in both x and y directions, and found that, in the light source coordinate system, the tilt of the surface was the same as the angle of the intensity gradient. This result was obtained by approximating the local surface with a spherical patch. The slant of

*This work was supported by NSF grants CDA-9122006 and CDA-9222798.

the surface was estimated using the assumption that the surface has uniform reflectance, and the brightest point on the surface has its normal pointing in the light source direction. The disadvantage of this approach is its limitation to spherical surfaces.

Another approach by Pentland [12] linearized the reflectance map in terms of the surface gradient, through the Taylor's series. By taking the Fourier transform of the linearized brightness equation and considering the relationship between the Fourier transform of the surface gradient and the Fourier transform of the height, the height can be recovered using the inverse Fourier transform of the intensity. Since no smoothness constraint is needed, this algorithm is applicable to complex natural surfaces. However, it has problems with images of quadratic and higher order surface reflectance because of the linearization of the reflectance map.

Instead of linearizing the reflectance map in terms of the gradient, Tsai & Shah [17] employed a discrete approximation to the gradient first, then linearized the reflectance map in terms of the height. Consequently, at each pixel, the intensity could be expressed by a linear function of the height at neighboring pixels, and the Jacobi iterative scheme could be applied to solve the entire linear system. This algorithm breaks down when self-shadows exist in the image.

Although local approaches are simple and fast, they have limitations, especially in the case of noisy real images. Therefore, several SFS algorithms use global information to ensure robustness.

The first two global approaches were by Ikeuchi & Horn [6], and Brooks & Horn [2]. Both combined the brightness constraint and the smoothness constraint to form an error function, then minimized it using variational calculus. In his later approach, Horn [5] added the integrability constraint to the error function. To solve the problem of slow convergence for Horn's approach, Szeliski [15] used the hierarchical and preconditioned conjugate gradient descent method to improve the efficiency. Unlike the above algorithms, which involve the recovery of either the surface normal or the surface gradient, Leclerc & Bobick [7] used a discrete approximation of the surface gradient to introduce height into the error function, which consists of the brightness constraint and the smoothness constraint. Then they directly solved for height by taking the derivative of the error function and applying a conjugate gradient technique. All of the above techniques require known shape information at occluding boundaries in order to enforce correct convergence. Leclerc & Bobick's approach needs the height output from stereo as the initial estimate.

Zheng & Chellappa [18] were the first to consider the first derivative of intensity in the variational calculus approach. However, their derivatives were taken along the x and y directions. Their error function contains the brightness constraint, the brightness derivative constraint, and the integrability constraint. For smooth Lambertian surfaces, since the change of intensity is small, the brightness constraint in their error function still dominates. The Taylor's series was applied to linearize the reflectance map, and discrete approximations for surface gradients, and their derivatives, were used. The iterative scheme was implemented using a hierarchical structure to solve for surface height and gradient simultaneously. The initial values for the height and gradient could be zero.

Lee & Kuo's approach [9] involves the brightness and smoothness constraints. The linearization of the reflectance map was combined with the triangularization of the surface to express the reflectance map as a linear function of the height. A quadratic error function was minimized by solving a sparse linear system. The multigrid method, with successive linearization, was used to solve this linear system. All height values could be initialized to zero.

Both Zheng & Chellappa's method and Lee & Kuo's method can recover good low frequency information, but high frequency information, the details, are smoothed out. Zheng & Chellappa's results are affected by the background value. Lee & Kuo's method tends to oversmooth the surface and the recovered height is slanted upward in one direction.

Another approach is by Dupuis and Oliensis [3, 10, 11]. Oliensis [10] observed that the smoothness constraint is only needed at the boundaries if we have initial values at the singular points. Based on this basic idea, Dupuis and Oliensis [3, 11] developed an iterative algorithm to recover depth using discretized optimal control and dynamic programming. The proof of equivalence between the optimal control representation and SFS was illustrated. Their initial algorithm [3] requires priori depth information for all singular points. A later extension [11] can determine this information automatically by assuming twice differentiable depth, isolated singular points and nonzero curvature at singular points.

Bichsel and Pentland [1] simplified Dupuis and Oliensis's approach. They found that a minimum downhill principle could remove the ambiguity introduced by singular points, so that the height information at singular points can be propagated to build a continuous surface. The propagation follows the

principle that the height information is only passed to pixels that are farther away from the light source. Among all the pixels that are farther away from the light source, choose the one that is the closest. This approach used the concept of the derivative of the reflectance map with respect to q, but, it does not directly use the intensity gradient information. The problem with this method is that it has difficulty with multiple singular points and is sensitive to noise.

Common problems among existing SFS algorithms include oversmoothing, lack of robustness, and excessive execution time. To overcome these problems, we introduce a new SFS algorithm, which follows the traditional global approach, but provides more realistic and reliable results.

3 Shape Extraction Using the Intensity Gradient

In our approach, we use neither the spherical assumption as in Lee & Rosenfeld's and Pentland's approaches, nor do we base our algorithm on singular points. Unlike Zheng and Chellappa's approach, which considered the intensity derivatives in the x and y directions, the brightness constraint, and the integrability constraint, we replace the traditional brightness constraint with an intensity gradient constraint. The direction of the intensity gradient is the direction in which the shape of the surface changes the most, therefore, this direction provides the most information. The directional derivative of the reflectance map, rather than the reflectance map, is linearized using Taylor's series. The discretization of both the surface gradient and its directional derivative, in terms of height, is used in order to express the derivative of the reflectance map as a linear function of height at neighboring pixels. To enforce a unique solution, the smoothness constraint, instead of the integrability constraint, is applied. The resulting nonlinear error function, which includes the smoothness constraint and the simplified intensity gradient constraint, is minimized through the solution of a sparse linear system, which is solved by the multigrid technique.

We use the traditional Lambertian model, based on the assumption of an infinite point light source:

$$I_{i,j} = R_{i,j} = \frac{(-p_{i,j}, -q_{i,j}, 1) \cdot \vec{S}}{\sqrt{p_{i,j}^2 + q_{i,j}^2 + 1}}, \qquad (1)$$

where $I_{i,j}$ is the input intensity at pixel (i,j), which is equal to the reflectance map $R_{i,j}$, $(p_{i,j}, q_{i,j})$ is the surface gradient, and $\vec{S} = (S_x, S_y, S_z)$ is the unit light source direction. We then take the directional derivative of the reflectance map along the intensity gradient direction $d_{i,j}$:

$$\begin{aligned} R_{d_{i,j}} &= \{(-S_x p_{d_{i,j}} - S_y q_{d_{i,j}})(p_{i,j}^2 + q_{i,j}^2 + 1) \\ &\quad -(S_z - S_x p_{i,j} - S_y q_{i,j})(p_{i,j} p_{d_{i,j}} + q_{i,j} q_{d_{i,j}})\} \\ &\quad / \{(p_{i,j}^2 + q_{i,j}^2 + 1)^{\frac{3}{2}}\}, \end{aligned} \qquad (2)$$

where $p_{d_{i,j}}$ and $q_{d_{i,j}}$ are the directional derivatives of $p_{i,j}$ and $q_{i,j}$ along the intensity gradient direction.

The first order Taylor's expansion around the fixed point $(\bar{p}_{i,j}, \bar{q}_{i,j}, \bar{p}_{d_{i,j}}, \bar{q}_{d_{i,j}})$ yields the following linear approximation to the directional derivative:

$$\begin{aligned} R_{d_{i,j}} &\approx R_{d_{i,j}}(\bar{p}_{i,j}, \bar{q}_{i,j}, \bar{p}_{d_{i,j}}, \bar{q}_{d_{i,j}}) \\ &\quad + \frac{\partial R_{d_{i,j}}}{\partial p_{d_{i,j}}}(p_{d_{i,j}} - \bar{p}_{d_{i,j}}) + \frac{\partial R_{d_{i,j}}}{\partial q_{d_{i,j}}}(q_{d_{i,j}} - \bar{q}_{d_{i,j}}) \\ &\quad + \frac{\partial R_{d_{i,j}}}{\partial p_{i,j}}(p_{i,j} - \bar{p}_{i,j}) + \frac{\partial R_{d_{i,j}}}{\partial q_{i,j}}(q_{i,j} - \bar{q}_{i,j}), \end{aligned} \qquad (3)$$

By rewriting equation (3), we obtain:

$$\begin{aligned} R_{d_{i,j}} &\approx \alpha_{i,j} p_{i,j} + \beta_{i,j} q_{i,j} + \gamma_{i,j} p_{d_{i,j}} \\ &\quad + \phi_{i,j} q_{d_{i,j}} + \eta_{i,j}, \end{aligned} \qquad (4)$$

$$\alpha_{i,j} = \frac{\partial R_{d_{i,j}}}{\partial p_{i,j}}, \qquad \beta_{i,j} = \frac{\partial R_{d_{i,j}}}{\partial q_{i,j}},$$

$$\gamma_{i,j} = \frac{\partial R_{d_{i,j}}}{\partial p_{d_{i,j}}}, \qquad \phi i,j = \frac{\partial R_{d_{i,j}}}{\partial q_{d_{i,j}}},$$

$$\begin{aligned} \eta_{i,j} &= R_{d_{i,j}}(\bar{p}_{i,j}, \bar{q}_{i,j}, \bar{p}_{d_{i,j}}, \bar{q}_{d_{i,j}}) - \alpha_{i,j}\bar{p}_{i,j} - \beta_{i,j}\bar{q}_{i,j} \\ &\quad - \gamma_{i,j}\bar{p}_{d_{i,j}} - \phi_{i,j}\bar{q}_{d_{i,j}}. \end{aligned}$$

We use the following discrete approximations for $p_{i,j}$, $q_{i,j}$, and their derivatives:

$$\begin{aligned} p_{i,j} &= z_{i,j} - z_{i,j-1}, \\ q_{i,j} &= z_{i,j} - z_{i+1,j}, \\ p_{x_{i,j}} &= z_{i,j} - 2z_{i,j-1} + z_{i,j-2}, \\ p_{y_{i,j}} &= z_{i,j} - z_{i,j-1} - z_{i+1,j} + z_{i+1,j-1}, \\ q_{x_{i,j}} &= z_{i,j} - z_{i+1,j} - z_{i,j-1} + z_{i+1,j-1}, \\ q_{y_{i,j}} &= z_{i,j} - 2z_{i+1,j} + z_{i+2,j}, \\ p_{d_{i,j}} &= p_{x_{i,j}} \Delta x_{i,j} + p_{y_{i,j}} \Delta y_{i,j}, \\ q_{d_{i,j}} &= q_{x_{i,j}} \Delta x_{i,j} + q_{y_{i,j}} \Delta y_{i,j}, \end{aligned}$$

where $p_{x_{i,j}}$ and $q_{x_{i,j}}$ are derivatives in the x direction, $p_{y_{i,j}}$ and $q_{y_{i,j}}$ are derivatives in the y direction, $\Delta x_{i,j} = \cos\theta$, and $\Delta y_{i,j} = \sin\theta$ (θ is the angle of the intensity gradient at pixel (i,j)). Then equation (4) can be expressed as a linear function of the height at neighboring points:

$$\begin{aligned} R_{d_{i,j}} &\approx \alpha_{i,j}(z_{i,j} - z_{i,j-1}) + \beta_{i,j}(z_{i,j} - z_{i+1,j}) \\ &\quad + \gamma_{i,j}[(z_{i,j} - 2z_{i,j-1} + z_{i,j-2})\Delta x_{i,j} \\ &\quad + (z_{i,j} - z_{i,j-1} - z_{i+1,j} + z_{i+1,j-1})\Delta y_{i,j}] \\ &\quad + \phi_{i,j}[(z_{i,j} - z_{i+1,j} - z_{i,j-1} + z_{i+1,j-1})\Delta x_{i,j} \\ &\quad + (z_{i,j} - 2z_{i+1,j} + z_{i+2,j})\Delta y_{i,j}] + \eta_{i,j}. \end{aligned} \qquad (5)$$

Now compute the height, $z_{i,j}$, by minimizing

$$\sum_{i,j=0}^{n-1}\{(I_{d_{i,j}} - R_{d_{i,j}})^2 + \lambda(p_{x_{i,j}}^2 + p_{y_{i,j}}^2 + q_{x_{i,j}}^2 + q_{y_{i,j}}^2)\}, \quad (6)$$

where, n is the image size, and λ is the weight of the smoothness term. The first term is the intensity gradient constraint, and the second term is the smoothness constraint. Substituting $R_{d_{i,j}}$ from equation (5) for the first term of (6), we obtain:

$$\begin{aligned}\sum_{i,j=0}^{n-1}\{&a_{i,j}^2 z_{i,j}^2 + b_{i,j}^2 z_{i,j-1}^2 + c_{i,j}^2 z_{i+1,j}^2 + d_{i,j}^2 z_{i,j-2}^2 + \\ &e_{i,j}^2 z_{i+1,j-1}^2 + f_{i,j}^2 z_{i+2,j}^2 + 2[a_{i,j}b_{i,j}z_{i,j}z_{i,j-1} + \\ &a_{i,j}c_{i,j}z_{i,j}z_{i+1,j} + a_{i,j}d_{i,j}z_{i,j}z_{i,j-2} + \\ &a_{i,j}e_{i,j}z_{i,j}z_{i+1,j-1} + a_{i,j}f_{i,j}z_{i,j}z_{i+2,j} + \\ &b_{i,j}c_{i,j}z_{i,j-1}z_{i+1,j} + b_{i,j}d_{i,j}z_{i,j-1}z_{i,j-2} + \\ &b_{i,j}e_{i,j}z_{i,j-1}z_{i+1,j-1} + b_{i,j}f_{i,j}z_{i,j-1}z_{i+2,j} + \\ &c_{i,j}d_{i,j}z_{i+1,j}z_{i,j-2} + c_{i,j}e_{i,j}z_{i+1,j}z_{i+1,j-1} + \\ &c_{i,j}f_{i,j}z_{i+1,j}z_{i+2,j} + d_{i,j}e_{i,j}z_{i,j-2}z_{i+1,j-1} + \\ &d_{i,j}f_{i,j}z_{i,j-2}z_{i+2,j} + e_{i,j}f_{i,j}z_{i+1,j-1}z_{i+2,j} + \\ &a_{i,j}g_{i,j}z_{i,j} + b_{i,j}g_{i,j}z_{i,j-1} + c_{i,j}g_{i,j}z_{i+1,j} + \\ &d_{i,j}g_{i,j}z_{i,j-2} + e_{i,j}g_{i,j}z_{i+1,j-1} + f_{i,j}g_{i,j}z_{i+2,j}] \\ &+g_{i,j}^2\}, \end{aligned} \quad (7)$$

where

$$\begin{aligned} a_{i,j} &= -\alpha_{i,j} - \beta_{i,j} - \gamma_{i,j}(\Delta x_{i,j} + \Delta y_{i,j}) \\ &\quad -\phi_{i,j}(\Delta x_{i,j} + \Delta y_{i,j}), \\ b_{i,j} &= \alpha_{i,j} + \gamma_{i,j}(2\Delta x_{i,j} + \Delta y_{i,j}) + \phi_{i,j}\Delta x_{i,j}, \\ c_{i,j} &= \beta_{i,j} + \gamma_{i,j}\Delta y_{i,j} + \phi_{i,j}(\Delta x_{i,j} + 2\Delta y_{i,j}), \\ d_{i,j} &= -\gamma_{i,j}\Delta x_{i,j}, \quad e_{i,j} = -\gamma_{i,j}\Delta y_{i,j} - \phi_{i,j}\Delta x_{i,j}, \\ f_{i,j} &= -\phi_{i,j}\Delta y_{i,j}, \quad g_{i,j} = I_{d_{i,j}} + \eta_{i,j}. \end{aligned}$$

The second term of equation (6), the smoothness constraint, can be represented by a template, to be applied to the 2-D height, as follows [9, 16]:

$$V : \frac{1}{h^2}\begin{vmatrix} & & 1 & & \\ & 2 & -8 & 2 & \\ 1 & -8 & 20 & -8 & 1 \\ & 2 & -8 & 2 & \\ & & 1 & & \end{vmatrix}. \quad (8)$$

Here, h is the spacing between pixels. The templates for the image boundary can be found in [9, 16].

Equation (7) can be rewritten in a matrix form:

$$\frac{1}{2}z^T U z - \omega^T z + \mu.$$

Adding the smoothness term (8) to this quadratic equation, we have:

$$\frac{1}{2}z^T T z - \omega^T z + \mu, \quad (9)$$

where $T = U + \lambda V$. U is an $n^2 \times n^2$ symmetric, sparse banded matrix consisting of the second order terms of (7).

The vector ω is an $n^2 \times 1$ vector consisting of the first order terms of (7). Finally, μ is a scalar consisting of the sum of the constant terms of (7):

$$\mu = \sum_{i,j=0}^{n-1} g_{i,j}^2.$$

The minimization of expression (9) is done by solving the linear system $Tz = \omega$.

4 Multigrid Technique

The basic idea behind the multigrid method is to combine a traditional relaxation method with coarse-grid correction, so that the error generated in the finer grid can be corrected in the coarser grid to yield a more efficient, and accurate, solution. The number of grid levels, L, in one iteration of the multigrid method is determined by the size of the image, n, to be $L = \log_2 n - 1$. The multigrid method can be performed iteratively by using the solution from the previous iteration as the initial value for the next. One iteration of the multigrid method, from the finest grid to the coarsest and back to the finest, is called a cycle. There are different structures for the cycle [14]. We use the V-cycle structure.

In our multigrid implementation, Gauss-Seidel was used for both the relaxation method and exact solver. Full-weighting restriction was applied to transfer the residual from finer grids to coarser grids, and bi-linear prolongation was applied to make the correction from coarser grids to finer grids. At each level, the size of the grid is reduced by half.

5 Results

Among existing SFS techniques, Lee & Kuo's approach provides very good results. They also applied the multigrid technique, therefore, we implemented their algorithm and compared the results with ours.

The results for our algorithm are given after one multigrid cycle; since the results after one cycle are already accurate enough, any extra cycles would not yield any significant improvement. However, the property of coarse-to-fine-correction in the multigrid technique makes even one cycle meaningful. The smooth-

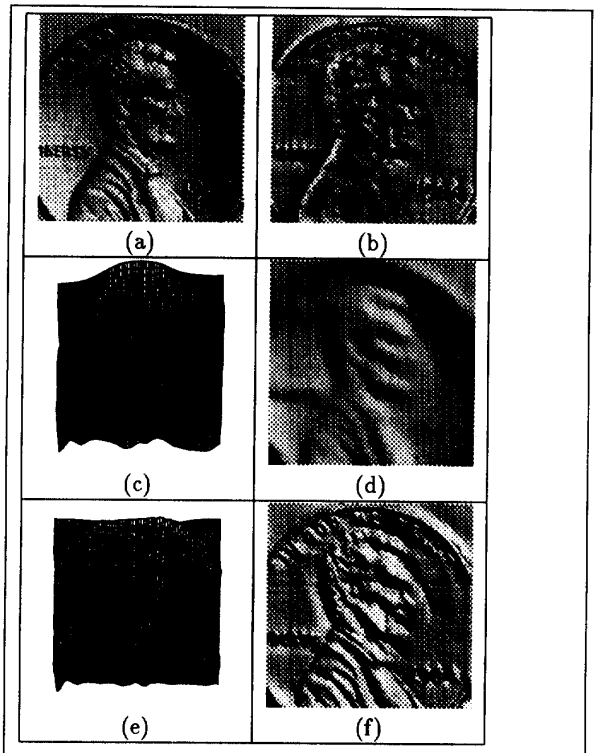

Figure 1: Results for *Penny*. (a) The input *Penny* image with light source $(5, 5, 7)$. (b) Shaded image for our output using light source $(-5, 5, 7)$. (c)-(d) 3-D plot of the recovered depth from Lee and Kuo's algorithm and its shaded image using light source $(5, 5, 7)$. (e)-(f) 3-D plot of the recovered depth from our algorithm and its shaded image using light source $(5, 5, 7)$.

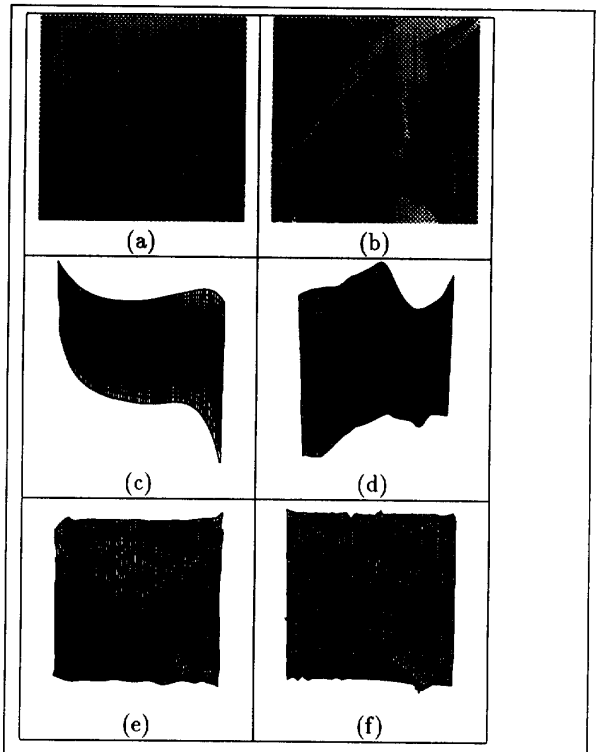

Figure 2: Results for real images. (a) *David* (the estimated light source direction is $(-0.707, 0.707, 1)$). (b) *Lenna* (the estimated light source direction is $(1.5, 0.866, 1)$). (c)-(f) 3-D plots of the recovered height from Lee & Kuo's algorithm ((c),(d)), and from our algorithm ((e),(f)).

Table 1: CPU time (in seconds)

	Images		
Methods	**Penny**	**David**	**Lenna**
Lee & Kuo	2678.29	1077.22	14546.79
Proposed method	374.37	814.39	1215.19

ing factor λ was chosen as 2000. The maximum number of iterations for Gauss-Seidel is 500. The initial heights were chosen as zero for all tests.

The results of the proposed algorithm are shown for one synthetic image *Penny* with light source $(5, 5, 7)$, and two real images with the light source directions estimated by Lee & Rosenfeld's method [8]: *Lenna* (the estimated light source direction is $(1.5, 0.866, 1)$), and *David* (the estimated light source direction is $(-0.707, 0.707, 1)$). The results for Lee & Kuo's algorithm, and for our own algorithm, are shown in Figures 1 and 2.

For *Penny*, Lee and Kuo's method loses a lot of detail, which causes the shaded output image to appear blurry. Moreover, the 3-D plot shows that their algorithm recovers a twisted background of the penny. On the other hand, our algorithm does not seem to exhibit any of these problems. The mean surface gra-

dient error is 1.14 for Lee and Kuo's algorithm and 0.47 for ours.

For *David*, the recovered height from Lee & Kuo's algorithm is very flat, even for small λ values. In contrast, our algorithm gives very good, detailed height information. Lee and Kuo's algorithms recovered very good height information for the real image *Lenna*, but, details are missing. Our result for *Lenna* shows accurate details. The rough height recovered in the area of Lenna's hair is due to the change in albedo, which violates the constant albedo assumption.

Although both Lee and Kuo's and our algorithms employ the multigrid technique, our method is significantly faster than Lee & Kuo's, no matter what threshold is used for Gauss-Seidel. This can be seen in Table 1. The analysis was done using a Sun SPARC 4.

In general, derivatives are sensitive to noise. However, our results for real images have shown that if we consider the derivative along the intensity gradient direction, the sensitivity to noise can be greatly reduced, with the help of regularization.

6 Conclusions

We presented a new SFS algorithm, which replaced the traditional brightness constraint with an intensity gradient constraint based on the fact that the direction of the intensity gradient is the direction in which the shape changes the most. The results have shown that our algorithm has robust performance for different real images, and that it is more efficient than the existing multigrid SFS technique.

Acknowledgements

Thanks to Prof. Kuo and Dr. Lee of USC for their helpful discussions and providing *Penny*, *Lenna*, and *David* images.

References

[1] M. Bichsel and A. P. Pentland. A simple algorithm for shape from shading. *CVPR*, pages 459–465, 1992.

[2] M. J. Brook and B. K. P. Horn. Shape and source from shading. *Proc. of International Joint Conference on Artificial Intelligence*, pages 932–936, 1985.

[3] P. Dupuis and J. Oliensis. Direct method for reconstructing shape from shading. *CVPR*, pages 453–458, 1992.

[4] B. K. P. Horn. *Shape from Shading: A Method for Obtaning the Shape of a Smooth Opaque Object from One View.* PhD thesis, MIT, 1970.

[5] B. K. P. Horn. Height and gradient from shading. *IJCV*, pages 37–75, 1989.

[6] K. Ikeuchi and B.K.P. Horn. Numberical shape from shading and occluding boundaries. *Artifical Intelligence*, 17(1-3):141–184, 1981.

[7] Y. G. Leclerc and A. F. Bobick. The direct computation of height from shading. *CVPR*, pages 552–558, 1991.

[8] C.H. Lee and A. Rosenfeld. Improved methods of estimating shape from shading using the light source coordinate system. *Artifical Intelligence*, 26:125–143, 1985.

[9] K. M. Lee and C. C. J. Kuo. Shape from shading with a linear triangular element surface model. *PAMI*, 15(8):815–822, 1993.

[10] J. Oliensis. Shape from shading as a partially well-constrained problem. *CVGIP: IU*, 54:163–183, 1991.

[11] J. Oliensis and P. Dupuis. A global algorithm for shape from shading. *ICCV*, pages 692–701, 1993.

[12] A. Pentland. Shape information from shading: a theory about human perception. *ICCV*, pages 404–413, 1988.

[13] A. P. Pentland. Local shading analysis. *PAMI*, 6:170–187, 1984.

[14] W. H. Press, B. P. Flannery, S. A. Teukolsky, and W. T. Vetterling. *Numerical Recipes in C.* Cambridge University Press, 1990.

[15] R. Szeliski. Fast shape from shading. *CVGIP: IU*, 53:129–153, 1991.

[16] D. Terzopoulos. Multilevel computational processes for visual surface resconstruction. *CVGIP*, 24:52–96, 1988.

[17] P. S. Tsai and M. Shah. A simple shape from shading algorithm. *CVPR*, pages 734–736, 1992.

[18] Q. Zheng and R. Chellappa. Estimation of illuminant direction, albedo, and shape from shading. *PAMI*, 13(7):680–702, 1991.